

Note also that the dependence of A, L, T on the choice of the range of p may be used to increase the accuracy of the results in the range of Fo which is of interest.

NOTATION

p, parameter of Laplace transformation; $\Phi(p)$, approximating function; A, L, T, parameters of approximation; τ , time; $\phi(t)$, inverse of $\Phi(p)$; $\theta(x, \tau)$ dimensionless temperature; $\Theta(x, p)$, transform of dimensionless temperature; $f(\tau)$, temperature at plate surface; $\bar{f}(p)$, transform of $f(\tau)$; Fo, Fourier number; ε , error of approximation; $\Gamma(L)$, gamma function.

LITERATURE CITED

1. A. I. Orurk, New Methods of Synthesizing Linear and Some Nonlinear Dynamic Systems [in Russian], Moscow (1965).
2. A. S. Trofimov, Inzh.-fiz. Zh., 49, 671-675 (1985).
3. A. S. Trofimov, A. V. Kozlov, E. Yu. Kovalenko, and E. M. Satsko, Inzh.-fiz. Zh., 49, No. 3, 513 (1985); Paper 2299-85 Deposited at VINITI [in Russian], Moscow (1985).
4. A. S. Trofimov and S. A. Pas', Inzh.-fiz. Zh., 52, No. 6, 1021 (1989); Paper 8186-V86 Deposited at VINITI [in Russian], Moscow (1986).
5. A. V. Lykov, Theory of Thermal Conductivity [in Russian], Moscow (1967).
6. M. Abramovits and I. Stigan (eds.), Handbook on Special Functions [in Russian], Moscow (1979).

NUMERICAL INVESTIGATION OF THE PROCESS OF VENTILATIVE DRYING OF A PIPELINE

V. M. Gorislavets and A. A. Sverdlov

UDC 622.692.4

A procedure for calculating the process of drying a pipeline with a desiccant is described that enables one to predict the time required for the complete removal of moisture. The influence of various factors on the rate of the process is analyzed without allowance for the temperature drop due to the heat consumed in evaporation.

Before putting into operation the pipelines designed for transporting high-quality petroleum products, as well as for supplying carbon dioxide to strata, it is necessary to dry the inner surface of the pipeline. (Otherwise, hydrates of hydrocarbons may form, resulting in obstruction of the pipes, measurement instruments, valves, etc., and hence in failures.) In the transportation of jet fuel, the presence of moisture is entirely unacceptable. The standard of the Petroleum Institute of the USA, for example, establishes a molar concentration of moisture in jet engine fuel of about 15 parts per million. A special feature of pipelines for pumping CO₂ is the need to carefully rid them of traces of water after a hydraulic test, since highly corrosive carbonic acid is formed in the interaction of CO₂ with water.

Most of the water that remains in a pipeline after a hydraulic test can be removed by successively passing a series of cylindrical or spherical inserts through the pipeline. After this operation, a small amount of water usually remains on the inner surface of the pipeline (the thickness of the water film may range from 50 to 100 μm), which can be removed by: a) ventilative drying; b) vacuum drying; c) absorptive drying.

In the present paper we investigate the process of ventilative drying (a fairly common means of removing moisture by means of a desiccant passed through the pipeline for a certain time). Air can be used as the desiccant in this case (it is exhausted directly into the atmosphere at the exit from the pipe, and at the entrance it is dehydrated and compressed) or another dry gas. A pipeline is considered to be ready for operation if the water vapor concentration in the desiccant at the exit from the pipe reaches a given minimum value;

All-Union Oil and Gas Scientific Research Institute, Kiev Branch. Translated from Inzhenerno-fizicheskii Zhurnal, Vol. 60, No. 5, pp. 804-813, May, 1991. Original article submitted December 18, 1989.

this requires a certain time that depends on the length of the pipeline, the flow rate of desiccant, its temperature, initial moisture content, etc.

MATHEMATICAL MODEL

The problem of drying a pipeline with a gaseous desiccant can be formulated as a problem of convective heat and mass transfer in the turbulent flow of a purely viscous fluid in a pipe. The process of drying with dry gas can be represented schematically by introducing some simplifications, which are justified by the fact that the mass concentration of water vapor in the desiccant remains very low. In particular, we assume that:

- a) the desiccant behaves like an ideal gas, i.e., we can assume, with sufficient accuracy for engineering calculations, that the gas containing moisture obeys all the laws of ideal gases;
- b) the pressure profile along the pipe can be calculated just as in the case of gas flow in the absence of moisture evaporation from the walls;
- c) all the terms pertaining to water vapor in the energy equation written for the gas-vapor mixture, as well as the terms allowing for kinetic energy and the action of gravity, can be neglected.

With allowance for the foregoing, the following system of equations describing the process of drying of a pipeline was obtained in [1]:

$$\frac{\partial W}{\partial \tau} = -Iq, \quad (1)$$

$$A\rho \frac{\partial C^*}{\partial \tau} = -G \frac{\partial C^*}{\partial x} + Iq, \quad (2)$$

$$C_v A\rho \frac{\partial T}{\partial \tau} = -C_p G \frac{\partial T}{\partial x} - LIq + \pi D\alpha(T_w - T), \quad (3)$$

$$\pi C_F D_{av} S \rho_F \frac{\partial T_w}{\partial \tau} = \frac{T_e - T_w}{R} - \pi D\alpha(T_w - T). \quad (4)$$

Even under the adopted assumptions, the problem of ventilative drying of a pipeline thus reduces to a fairly unwieldy system of partial differential equations, to solve which one must determine the variation of W , C^* , T , and T_w along the length of the pipeline at each time. Here one must remember that the limiting allowable concentration of water vapor in the desiccant is determined by the vapor pressure, which depends on the temperature of the desiccant, i.e., in addition to the indicated quantities, each time one must find P_s along the length of the pipeline, which is calculated from the formula [2]

$$\begin{aligned} \log(P_s) = & -3,142305 \left[\frac{10^3}{T + 273,16} - \frac{10^3}{373,16} \right] + \\ & + 8,21 \log \left(\frac{373,16}{T + 273,16} \right) - 0,0024804 [373,16 - (T + 273,16)]. \end{aligned} \quad (5)$$

In the first stage of the present investigation, we confined ourselves to solving the system (1), (2), i.e., we neglected the influence of the temperature drop of the desiccant due to moisture evaporation from the pipeline walls on the drying time.

In such a formulation, for system (1), (2) we can specify the initial conditions

$$\begin{aligned} C^*(x, \tau) &= C^*(x, 0) = C_0^*, \\ W(x, \tau) &= W(x, 0) = W_0, \end{aligned} \quad (6)$$

$$\begin{aligned} q(x, \tau) &= q(x, 0) = 0, \\ T(x, \tau) &= T(x, 0) = T_e \end{aligned}$$

and the boundary conditions

$$C^*|_{x=0} = C_{en}^* = \text{const}, \quad (7)$$

$$T|_{x=0} = T_{en} = T_e, \quad (8)$$

$$T|_{x=l} = T_{ex} = T_e. \quad (9)$$

Equations (1) and (2) express the law of conservation of water by mass in the liquid and vapor phases, respectively. The term I_q represents the mass of moisture converted to the vapor state per unit length of pipeline per unit time.

In the case of binary gaseous systems with one diffusing component, the best expression describing the rate of mass transfer in the saturated section is the equation given in [3]:

$$N_A = K^* \ln \left[\frac{1 - Y_A}{1 - Y_{A_1}} \right], \text{ mole}/(\text{sec} \cdot \text{cm}^2). \quad (10)$$

By analogy with Eq. (10), the mass flux of water vapor in the saturated section can be found from the equation

$$q = K_y \ln \left[\frac{1 - Y}{1 - Y_s} \right], \text{ kg}/(\text{h} \cdot \text{m}^2). \quad (11)$$

The molar content of moisture near the pipe wall is determined, in turn, as the limiting moisture content expressed in molar fractions [4]:

$$Y_s = \frac{P_s}{P - P_s}. \quad (12)$$

The mass yield coefficient K_y in Eq. (11) is determined from the expression [5]

$$K_y = \frac{0.023 MW_v D_{va}^0}{MW_a D} \left(\frac{v}{D_{va}} \right)^z \text{Re}^{0.8}. \quad (13)$$

The exponent z in Eq. (13) depends on the Reynolds number. For $\text{Re} > 10^4$, we can take $z = 1$. Equation (13) then takes the form

$$K_y = \frac{0.023 \eta}{D} \frac{MW_v}{MW_a} \text{Re}^{0.8}. \quad (14)$$

To use Eq. (11), it thus remains to determine the molar fraction Y of water vapor in the stream core. The latter can be determined from the equation [4]

$$Y = 1.61 C^* \quad (15)$$

in terms of the mass fraction C^* of water vapor in the stream core, which can be found, in turn, from the solution of the system (1), (2), and (6)-(9).

The problem under consideration was solved numerically by the method of finite differences [6].

In connection with the numerical solution of the Navier-Stokes equations in dynamic variables [7, 8], explicit and implicit schemes and schemes of variable directions and fractional steps have been studied [9, 10]. Explicit difference schemes are simpler and yet provide fairly rapid convergence to a steady-state solution for large Reynolds numbers; they are constructed in such a way that each differential equation is juxtaposed to two difference equations; the initial grid functions in each time layer are determined in two steps [11], i.e., for the model equation

$$\frac{\partial u}{\partial \tau} + a \frac{\partial u}{\partial x} = v \frac{\partial^2 u}{\partial x^2} + bu + N \quad (16)$$

this scheme has the form

$$\frac{\bar{u}_i^{k+1} - u_i^k}{m} + a \frac{u_{i+1}^k - u_{i-1}^k}{2h} = 0, \quad (17)$$

$$\begin{aligned} \frac{u_i^{k+1} - u_i^k}{m} = & \beta \left(-a \frac{\bar{u}_{i+1}^{k+1} - \bar{u}_{i-1}^{k+1}}{2h} + v \frac{\bar{u}_{i+1}^{k+1} + \bar{u}_{i-1}^{k+1} - 2\bar{u}_i^{k+1}}{h^2} \right) + \\ & + (1 - \beta) \left(-a \frac{u_{i+1}^k - u_{i-1}^k}{2h} + v \frac{u_{i+1}^k + u_{i-1}^k - 2u_i^k}{h^2} \right) + bu_i^k + N. \end{aligned} \quad (18)$$

An important feature of this scheme is that in using it, locations in computer memory must be assigned for the values of the unknown grid functions in only two time layers. Owing to this fact, the numerical solution of hydrodynamic problems on the same difference grid by the scheme (17), (18) requires two-thirds and half as much memory as solutions by the schemes of Brailovskaya and Chudov [8], respectively.

The parameter $\beta = 0$ is used in the scheme (18) to study flows at low Reynolds numbers. At large Reynolds numbers, preference must be given to the scheme (18) with $\beta = 1$, since the limits on the difference steps of the grid turn out to be less strict in this case.

An analysis of data on ventilative drying showed that a transitional or quadratic regime occurs [12], i.e., the scheme (18) with $\beta = 1$ must be used in our case.

In accordance with this scheme, the differential equation (2) is juxtaposed to two difference equations,

$$\frac{\bar{C}_i^{*k+1} - C_i^{*k}}{m} + a \frac{C_{i+1}^{*k} - C_{i-1}^{*k}}{2h} = 0 \quad (19)$$

and

$$\frac{C_i^{*k+1} - C_i^{*k}}{m} = -a \frac{\bar{C}_{i+1}^{*k+1} - \bar{C}_{i-1}^{*k+1}}{2h} + N, \quad (20)$$

where $a = G/A\rho$; $N = Iq/A\rho$.

The differential equation (1) corresponds to the difference equation

$$\frac{W_i^{k+1} - W_i^k}{m} = -Iq. \quad (21)$$

In the numerical solution of problems of the flow of a viscous fluid, the steps of the difference grid are chosen in accordance with the necessary conditions of stability, which are found by the conditional setting of certain unknown functions of the system. In those cases in which the thermophysical properties of the working medium are assumed to be constant, the desiccant behaves like an ideal gas, and the spatial steps are equal in all directions, for the time step we have [7]

$$m = \min \left\{ \frac{h}{|u| + |v| + |w|}, \frac{h^2}{\beta_1 \frac{\eta}{\rho}}, \frac{h^2}{\beta_2 \frac{\lambda}{\rho(C - R_g)}} \right\}. \quad (22)$$

Numerical solutions of a number of one-dimensional and two-dimensional problems of heat transfer in the flow of viscous fluids indicate that the necessary conditions for stability (22) are similar to the sufficient conditions.

Calculations showed that the time difference step, defined as

$$m = \frac{h}{|u|} \quad (23)$$

(since the flow is one-dimensional), is the minimum in our case.

It must be remembered, however, that in the case of ventilative drying, a special condition is imposed on Eq. (23), which limits the choice of the step h of the spatial partition. This is explained by the fact that near the entrance for the dry gas, evaporation of moisture from the pipe walls occurs very rapidly due to the large difference between the concentrations of water vapor near the pipe walls and in the core of the gas stream. And if a fairly large spatial step is chosen, the desiccant may already reach the saturated state in the first spatial step, and this may occur at any point of this step, i.e., at almost the very start, in the middle, or at the end of the first step (depending on the evaporation rate and the chosen length of the step). The spatial step must therefore be chosen so as to eliminate saturation being reached in the first step, at which the maximum evaporation rate occurs. On the other hand, to save computer time the spatial step must not be too small, either. We therefore formulate the special condition in the form

$$C_i^* = C_{s_i}^* \text{ for } i > 2, \quad (24)$$

where i is the serial number of the grid line.

The special condition (24) requires that the spatial step be chosen so that the desiccant entering the pipeline reaches the saturated state after traveling a distance equal to at least two spatial steps.

Not satisfying the condition (24) leads to results that differ severalfold from the actual values. At the same time, observing the condition (24) requires that a spatial step of

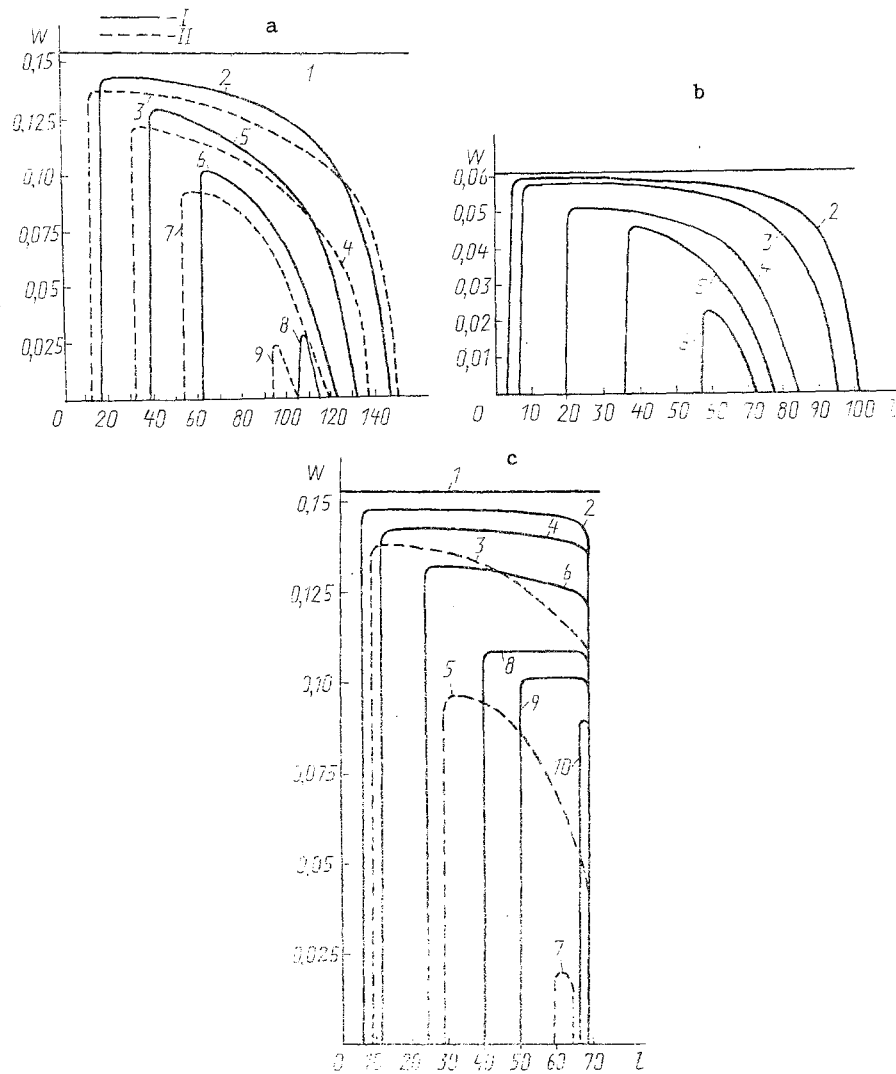


Fig. 1. Dynamic distribution of residual moisture along a pipeline [I) our data, II) data of [1]]: a) diameter 460 mm, length 156 km, temperature of dry air 15°C [1) $\tau = 0$; 2) $\tau = 58$ h; 3) 60; 4) 120; 5) 122; 6) 175; 7) 180; 8) 230; 9) 230]; b) 219 mm, 101 km, and 5°C, respectively [1) $\tau = 0$; 2) $\tau = 67$ h; 3) 125; 4) 320; 5) 452; 6) 570]; c) 530 mm, 69 km, and 3°C [1) $\tau = 0$; 2) $\tau = 65$ h; 3) 96; 4) 129; 5) 256; 6) 258; 7) 345; 8) 379; 9) 439; 10) 526]. W, kg/m; ℓ , km.

about 20-50 m be maintained, which, considering the length of pipelines, leads to a large number of spatial steps, and hence of time steps, i.e., to a large amount of computer time.

To reduce the computer time spent in calculating the process of drying a pipeline, we therefore used a nonuniform grid, i.e., in the section of the pipeline in which the air has not yet reached the saturated state we assign a "small" spatial step h_1 , satisfying the condition (24), and from this step we determine the time step from the condition (23). For the rest of the pipeline, to which Eqs. (1) and (2) do not extend, since gas saturated with water vapor flows there, we use a large spatial step h_2 , exceeding h_1 by a factor of 20-50 (it is usually chosen to be 1 km). The possibility of using such a large spatial step in this part of the pipeline is explained by the fact that here the absorption of water vapor occurs due to the increase in the concentration of saturated vapor in the air with greater distance from the entrance (in connection with the decrease in the head); the absorption is very small over a length h_1 (it is actually proportional to the difference between the saturation concentrations over the spatial step h_1) and differs as little over adjacent sections of the same length. The error in determining the mass of water evaporated from a unit length of pipeline on the spatial scales h_1 and h_2 over a time period corresponding to the time

TABLE 1. Main Characteristics of the Calculated Pipelines

Characteristics of pipelines	Figure number		
	1a	1b	1c
Pipeline length, km	156	101	69
Pipeline diameter, mm	460×19	219×9	530×11
Temperature, °C of ambient medium	15	5	3
of desiccant at pipe entrance	15	5	3
Desiccant flow rate, m ³ /h	10 000	2400	5000
Desiccant velocity, m/sec	20	19,6	6,85
Pressure, atm*			
at entrance	4,0	5,71	1,36
at exit	1,033	1,033	1,1

*1 atm = 10⁵ Pa.

TABLE 2. Results of Calculation

Figure number	Main characteristics				
	desiccant	initial amount of water, kg	dew point, °C	molar content of water in desiccant at entrance	drying time, h (days)
1, a	Air	24365*	-40	0,0001272	240 (10)
1, b	«	6161**	-50	0,00003655	590 (24,6)
1, c	Natural gas	10557*	-18	0,0011195	535 (22,3)

*Corresponds to a water film about 100 μm thick.

**Corresponds to a water film about 80 μm thick.

step m is therefore less than 1%. At the same time, the use of larger spatial steps in the part of the pipeline through which saturated gas flows enables us to reduce the calculation time manifold.

Equations (11) and (14) and the difference equations (19)-(21) thus extend to the initial drying section and "operate" until the desiccant reaches the saturated state. Over the rest of the pipeline the differential approach does not make sense, since here at each point of the pipeline the concentration of water vapor in the desiccant remains constant (assuming a constant temperature) and equal to the saturation concentration corresponding to each point of the pipeline and determined from Eq. (12). In this section of the pipeline, the flow of moisture removed from a unit length in a time step m is determined from the equation

$$\bar{W}_{h_2} = 0.804(Y_{s_{i+n}} - Y_{s_i}) Qm/h_2. \quad (25)$$

RESULTS OF THE CALCULATION

On the basis of the algorithm described above, we wrote a program and tested it in a calculation of the process of drying a pipeline with a diameter 460 × 19 mm and a length 156 km; the results of the calculation were given in [1]. The reliability of the data obtained is confirmed in a comparison of the graphs of the dynamics of drying, given in [1], with the results of our calculation (see Fig. 1a). As seen from Fig. 1a, the agreement is quite acceptable, especially if we consider that the results in Ref. 1 were obtained with allowance for the temperature drop in the sections in which the desiccant has not yet reached saturation.

In Fig. 1b and 1c we show the dynamics of ventilative drying of two other pipelines. All the data characterizing the calculated pipelines are given in Table 1. The results of the calculations are given in Table 2. Here it must be noted that all the calculations were made under the assumption that the water film is distributed uniformly over the surface of the pipe at each step analyzed. In the first two cases, the desiccant was dehydrated air, heated to the temperature of the ambient medium around the pipeline, i.e., to +15 and +5°C, respectively, and in the last case it was natural gas supplied to the pipe at +3°C. In all the figures it is shown how the drying process develops along the length of the pipe with time; it is seen that the end of the pipeline dries differently under these conditions.

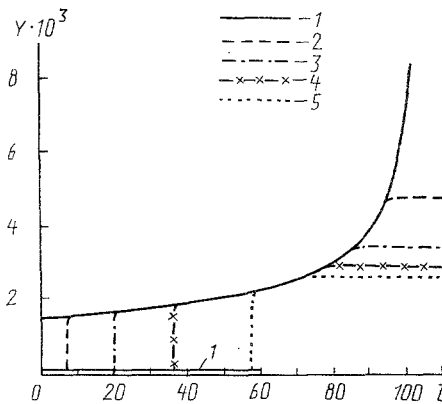


Fig. 2. Molar concentration of water vapor in air drying a pipeline 219 mm in diameter and 101 km long at different times: 1) at the pipe entrance; 2) $\tau = 125$ h; 3) 320; 4) 452; 5) 570. Y , molar fraction; l , km.

The results given in Fig. 1a confirm what was said earlier, that the drying process takes place from the ends toward the center of the pipeline. The same pattern is observed in Fig. 1b, but the drying process takes place far more slowly. If we consider that the air velocity is the same in the two cases (see Table 1), then it becomes clear at once that such a decrease in drying rate (see Table 2) is explained by the different air temperatures (15 and 5°C, respectively). At the same time, as seen from Fig. 1c, the end of the pipeline dries only at the end of the drying in this case (solid curve). This is explained by the combination of the low temperature of the natural gas and its low velocity (see Table 1) and is confirmed by the fact that doubling of the velocity of the desiccant (dashed curves) results in a considerable reduction in drying time (348 h as compared with 535 h), as well as the fact that about the last 5 km of the pipeline is able to dry before the drying process is completed.

It can be seen from Fig. 2 (it pertains to the pipeline for which the drying dynamics is shown in Fig. 1b), in turn, that the efficiency of the drying process decreases with time. Here the molar moisture content of the air at the exit from the pipe equals the saturation molar concentration under the conditions of the last dew point for the air involved.

We must discuss once again a peculiarity of the process of ventilative drying. As seen from Table 2, the drying time for the third pipeline is less than the drying time for the second, despite the fact that the second pipeline contained less water than the third and the desiccant temperatures differed insignificantly. Such "disagreement" is explained by the fact that the pressure at the entrance to the second pipeline (see Table 1) was more than four times the pressure at the entrance to the third pipeline, and this means that at the entrance to the third pipeline, in accordance with Eq. (12), the molar concentration of water vapor corresponding to the saturated state was considerably higher than for the second pipeline, i.e., the evaporation rate was far higher in the third pipeline. One must always remember this fact. It follows from it that the time required to dry a pipeline is shortened with increasing desiccant velocity only to a certain extent. A strong increase in velocity may lead to such an increase in pressure at the pipeline entrance that the moisture content of the desiccant in the saturated state decreases sharply, as a result of which the evaporation rate q is strongly reduced (at $Y_{en} = Y_{s1}$ it becomes equal to zero at the entrance, and for $Y_{en} > Y_{s1}$ it even becomes negative).

Our numerous calculations with variation of different parameters characterizing the drying process showed that the process of ventilative drying of a pipeline is, under certain conditions, a very competitive means of removing moisture remnants, since the equipment required is relatively inexpensive, does not require trained personnel, and can achieve a very high degree of drying. An accurate prediction of the drying process is required, however, to choose the optimum conditions.

An analysis of our calculated data shows that an optimum desiccant flow rate exists; the optimum is sought as a function of the diameter of the pipeline to be dried and the

initial moisture content of the desiccant. The calculated results show, in addition, that an optimum length of the section of pipeline to be dried exists from the standpoint of minimizing the drying time. As important as a reduction in drying time is, one must consider the consumption of desiccant and its cost. The computer program that we have developed enables one to obtain a fairly accurate picture of the drying process, which makes it possible, in turn, to optimize the main parameters.

The calculated time was compared with the experimental time obtained in drying the Berezniki-Ol'khovka carbon dioxide pipeline, with a diameter 219×9 mm and a length 101 km, for which dry air with a dew point -50°C and a flow rate $2400 \text{ m}^3/\text{h}$ was used as the desiccant. The experimental data differed from the calculations by 5-15% and confirmed the dynamics of the drying process obtained theoretically. One must bear in mind that allowing for the temperature drop of the desiccant in the evaporation sections enables one to predict the drying time more accurately, but it consumes more computer time. At the same time, neglecting this factor results in an error not exceeding 10% in determining the pipeline drying time, and the calculation time is an order of magnitude shorter.

NOTATION

W , mass of water per unit length of pipeline; I , transfer surface area at the air-water interface per unit length; q , mass of water evaporated per unit time from a unit of surface; τ , time; A , cross-sectional area of the pipeline; ρ , ρ_F , density of the desiccant and the pipe material, respectively; x , distance along the pipe; C^* , C_{en}^* , concentration of water vapor per unit mass of desiccant in the cross section under consideration and at the pipe entrance; G , mass flow rate of desiccant; C_v , C_p , specific heat of desiccant at constant volume and constant pressure; L , latent heat of evaporation of water; T , T_w , T_e , temperature of desiccant, pipe wall, and ambient medium; S , thickness of pipe wall; α , coefficient of heat transfer from desiccant to pipe; R , total resistance to heat transfer between pipe and ambient medium; P_s , P , saturation vapor pressure of water and desiccant pressure along the pipeline; l , length of pipeline; W_0 , initial mass of water per unit length of pipeline; N_A , molar flux of diffusing substance per unit time from a unit area; K^* , K_y , coefficient of mass transfer, expressed in terms of molar fractions and mass; Y_{A_1} , Y_A , molar fractions of the diffusing substance near the evaporation surface and in the stream core; Y , Y_s , concentration of water vapor in the desiccant in the stream core and near the pipe wall, expressed in molar fractions; η , ν , dynamic and kinematic viscosity of the coolant; MW_v , MW_a , molecular weight of water vapor and of the desiccant; D_{va} , coefficient of diffusion of water vapor in the desiccant; Re , Reynolds number; m , time step; h , spatial step; u , v , w , velocity components in the directions of the coordinate axes; λ , C , thermal conductivity and specific heat of desiccant; R_g , gas constant; $\beta_1 = 16/3, 28/3, \text{ and } 40/3$ and $\beta_2 = 4, 8, \text{ and } 12$ for the one-dimensional, two-dimensional, and three-dimensional problems; C_{s_i} , limiting concentration of water vapor per unit mass of desiccant in the respective cross section; Q , volumetric flow rate of desiccant; n , ratio of the large to the small spatial step; D , D_{av} , inside and average diameter of the pipeline; C_w , specific heat of the pipe material.

LITERATURE CITED

1. V. Battara, S. Selendari, and U. Bilardo, *Oil Gas J.*, **82**, No. 24, 114-116 (1984).
2. M. P. Vukalovich, *Thermodynamic Properties of Water and Steam* [in Russian], Moscow (1955).
3. T. K. Sherwood, R. L. Pigford, and C. R. Wilke, *Mass Transfer*, McGraw-Hill, New York (1975); 2nd ed. (1989).
4. V. A. Kirillin, V. V. Sychev, and A. E. Sheindlin, *Engineering Thermodynamics* [in Russian], Moscow (1974).
5. T. H. Cilton and A. P. Colburn, *Ind. Eng. Chem.*, **26**, No. 11, 1183-1187 (1934).
6. A. A. Samarskii, *Introduction to the Theory of Difference Schemes* [in Russian], Moscow (1977).
7. N. I. Nikitenko, *Investigation of Processes of Heat and Mass Transfer by the Grid Method* [in Russian], Kiev (1978).
8. I. Yu. Brailovskaya, A. L. Krylov, T. V. Kuskova, and L. A. Chudov, *Izv. Sib. Otd. Akad. Nauk SSSR, Ser. Tekh. Nauk, Part 2*, No. 8, 87-91 (1967).
9. V. M. Paskonov, V. I. Polezhaev, and L. A. Chudov, *Numerical Modeling of Processes of Heat and Mass Transfer* [in Russian], Moscow (1984).

10. I. S. Berezin and N. P. Zhidkov, Computing Methods [in Russian], Moscow (1966) [translated by O. M. Blunn, Pergamon Press, London (1965)].
11. N. I. Nikitenko, "Investigation of nonsteady processes of heat and mass transfer by the grid method," Author's abstract of dissertation for degree in engineering sciences, Kiev (1969).
12. P. N. Tugunov and V. F. Novoselov, Transport and Storage of Oil and Gas [in Russian], Moscow (1975).

A NEW TYPE OF SELF-EXCITED THERMOMECHANICAL OSCILLATIONS

S. E. Nesis and A. F. Shatalov

UDC 536.24

A new type of self-excited thermomechanical oscillations of heaters with ferromagnetic properties is investigated. The conditions for the onset of such self-excited oscillations are analyzed qualitatively.

Temperature oscillations (generated, e.g., by an alternating current) in a body are known to induce oscillations of the dimensions and shape of the heater, along with mechanical vibrations. Such hybrid oscillations are now known as thermomechanical oscillations (TMO). A special kind of self-excited thermomechanical oscillations (SETMO) can also arise in the system under certain conditions [1].

Here we give the results of investigations of a new type of SETMO observed in ferromagnetic heaters.

Since the magnetization I decreases abruptly with increasing temperature near the Curie point T_C (Fig. 1a), strong pulsations of I can be produced in a ferromagnet by exciting thermal oscillations in it. If a ferromagnetic vibrator is introduced into a static nonuniform magnetic field, it begins to be subjected to a force [2]

$$F = I \frac{dH}{dx},$$

which varies periodically because of the pulsations of I . Clearly, such a perturbing force can excite steady-state SETMO under certain conditions.

Inasmuch as the attractive force F can be directed only in the direction of increasing magnetic field H , the temperature of the ferromagnetic vibrator must decrease as the magnet comes closer and, conversely, it must increase as the magnet moves away in order for the mechanical vibrations to be amplified. It should also be borne in mind that the field H decays rapidly with increasing distance x ($dH/dx < 0$).

In the final analysis three conditions are required in order for strong SETMO to be generated: 1) The frequency ω of the temperature oscillations must be a multiple of the natural frequency ω_0 of the vibrator; 2) the time shift τ between the temperature and mechanical oscillations must be such that the temperature of the ferromagnet drops sharply as the vibrator approaches the magnet; 3) the amplitude θ of the thermal oscillations must be large enough for the energy input into the oscillatory system to cover dissipative losses.

We have observed SETMO of this kind experimentally, using a ferromagnetic vibrator with the configuration shown in Fig. 1c.

The vibrator comprised a lightweight mica frame mounted in needle bearings; the frame was capable of executing torsional vibrations. A nickel wire coil ($d = 10^{-4}$ m) was wound on one side of the frame in a bifilar configuration. The coil-wound frame was placed in the field of a permanent magnet, which was situated either to one side (position I) or underneath (position II) the coil.